

## BEAM DYNAMICS DESIGN ASPECTS FOR A PROPOSED 800 MEV H<sup>-</sup> ISIS LINAC

C. Plostinar, C. Prior, G. Rees, STFC/ASTeC, Rutherford Appleton Laboratory, UK

### Abstract

Several schemes have been proposed to upgrade the ISIS Spallation Neutron Source at Rutherford Appleton Laboratory (RAL) [1]. One scenario is to develop a new 800 MeV, H<sup>-</sup> linac and a ~3 GeV synchrotron, opening the possibility of achieving several MW of beam power. In this paper the design of the 800 MeV linac is outlined with an emphasis on the beam dynamics design philosophy. The linac consists of a 3 MeV Front End similar to the one now under construction at RAL (the Front End Test Stand -FETS). Above 3 MeV, a 324 MHz DTL will be used to accelerate the beam up to ~75 MeV. At this stage a novel collimation system will be added to remove the halo and the far off-momentum particles. To achieve the final energy, a 648 MHz superconducting linac will be employed using three families of elliptical cavities with transition energies at ~196 MeV and ~412 MeV.

Table 1: General Linac Parameters

Ion Species	H <sup>-</sup>
Output Energy	800 MeV
Accelerating Structures	DTL/SC Elliptical Cavities
Frequency	324/648 MHz
Beam Current	43 mA
Repetition Rate	30 Hz (Upgradeable to 50)
Pulse Length	0.75 ms
Duty Cycle	2.25 %
Average Beam Power	0.5 MW
Total Linac Length	243 m

beam between the linac and the ring. The main linac parameters are presented in Table 1 and a schematic overall layout in Figure 1 [2],[3],[4].

### THE FRONT END

The linac front end will consist of an H<sup>-</sup> ion source, a Low Energy Beam Transport Line (LEBT), an RFQ and a Medium Energy Beam Transport Line (MEBT) with a beam chopper [5].

The FETS Penning type surface plasma H<sup>-</sup> ion source will be adopted for the new linac. This source is already operating at parameters exceeding those required for the new linac having been improved over many years in ISIS and FETS. A beam of 65 keV, 1 ms at 50 Hz with beam currents exceeding 60 mA is routinely extracted.

A three solenoid magnetic LEBT will transport and match the beam from the ion source to the RFQ. A 4 m long, 4-vane RFQ operating at 324 MHz will accelerate the beam up to 3 MeV making use of the available 2.5 MW Toshiba klystron used at J-PARC. An RMS emittance in the region of 0.27 π mm mrad transversally and 0.39 π mm mrad longitudinally is expected at the output of the RFQ.

### DESIGN OVERVIEW

The design of the new linac follows the same overall guiding principles as several recent major proton/H<sup>-</sup> linac projects (ESS, J-PARC, Linac4/SPL, SNS). It consists of a 3 MeV front end copying the FETS project currently under construction at RAL. After 3 MeV, a DTL will accelerate the beam up to 74.8 MeV at which stage an intermediate energy beam transport line (IEBT) with an innovative collimation system will be used to remove the halo and the far off-momentum beam. Although this adds ~7.5 m to the overall linac length, hence increasing its cost, it is imperative to control the beam loss of quality ahead of the superconducting stages. The superconducting linac (SCL) uses 648 MHz cavities to accelerate the beam to 800 MeV with three families of elliptical cavities and transition energies at ~196 and ~412 MeV. A beam line of with achromatic bending sections is used to transport the

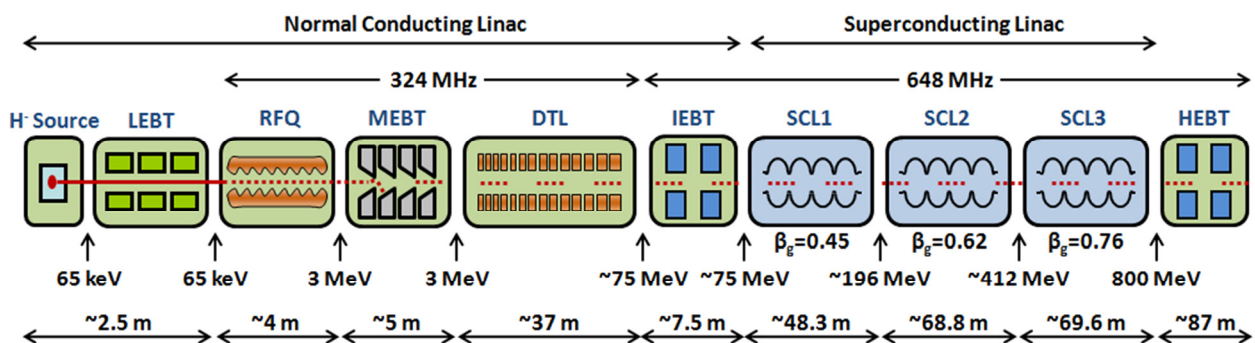


Figure 1: Schematic layout of the new 800 MeV ISIS Linac

Copyright © 2012 by the respective authors — cc Creative Commons Attribution 3.0 (CC BY 3.0)

The RFQ is followed by the MEFT line. It is nearly 5 m long and consists of 11 quadrupoles, 4 re-bunching cavities, a fast beam chopping system with dedicated beam dumps, collimators and a comprehensive set of diagnostics. The last 4 quadrupoles and buncher cavity form the section matching into the DTL.

### THE DTL AND IEFT

The DTL section is ~37 m long and accelerates the beam to 74.8 MeV in four tanks. Each tank is fed by a single 2.5 MW peak power Toshiba klystron with output energies of 19.4, 37.7, 56.4 and 74.8 MeV. The average axial electric field is ramped from 2.9 to 3.1 MV/m in the first tank and then kept constant.

A FODO focusing lattice is used throughout the linac. From a beam dynamics point of view, equipartitioning between the transverse and the longitudinal energies is obtained in the first tank after the MEFT matching section and is maintained up to 800 MeV by varying the quadrupole settings while keeping the transverse and longitudinal phase advances per period below 90 degrees. Figure 2 shows the zero current phase advance per period throughout the linac.

A large longitudinal acceptance is needed at the beginning of the DTL and as a result the synchronous phase angle ( $\phi_s$ ) is set to -42 degrees in the first few cells. As the beam becomes more bunched, the phase is slowly increased. Figure 3 shows the evolution of the synchronous phase throughout the linac. Transverse, inter-tank matching is done with six end quadrupoles while longitudinally, this is achieved by offsetting the synchronous phase in selected tank end cells.

A novel addition to the linac design is the inclusion of a collimation section (IEFT) at the end of the DTL. The IEFT is intended to limit the losses further downstream by intercepting halo and far off-momentum particles with stripping foils and loss collectors. Additionally, it facilitates the matching over a double frequency jump and accelerating structure change, providing ample space for diagnostic systems. Beam dynamics simulations indicate that the benefits of adding the IEFT in terms of beam quality outweigh the inherent overall cost increase.

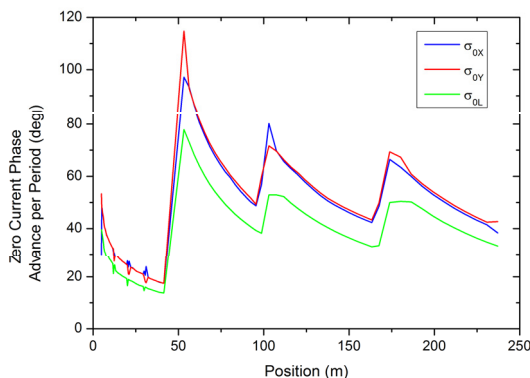


Figure 2: Linac zero current phase advance.

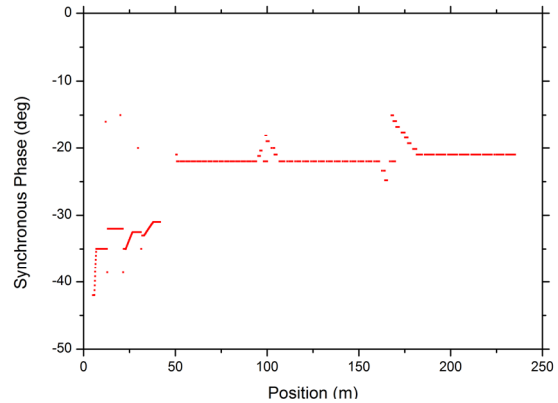


Figure 3: Synchronous phase evolution.

### THE SUPERCONDUCTING SECTION

After the IEFT, superconducting cavities are used to accelerate the beam to the final energy. The resonant frequency is doubled to 648 MHz in the SCL, mainly for cryogenic and manufacturing cost reasons. Acceleration is achieved in three stages with three cavity families ( $\beta_g=0.45, 0.62, 0.76$ ). Figure 4 shows the energy gain profile throughout the linac. The overall design aim has been to minimize the number of cavities and cryostats without compromising practical and beam dynamics design aspects. A list of parameters of the SCL is given in Table 2, while the configuration of the cryomodules can be seen in Figure 5.

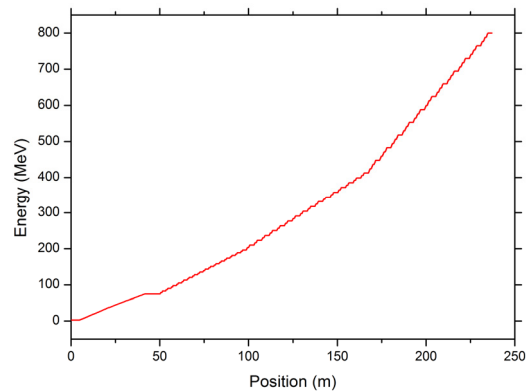


Figure 4: Linac energy profile.

Table 2: Superconducting linac parameters.

	SCL1	SCL2	SCL3
Energy (MeV)	~75-196	~196-412	~412-800
Cavity $\beta_g$	0.45	0.62	0.76
Cavity Length ( $\beta_g\lambda$ )	2	2.5	3
Cells per Cavity	4	5	6
$\Phi_s$ (deg)	-22	-22	-21
$E_{acc}$ (MV/m)	15.1-19.1	14.1-16.9	16.8-18.7
No. of Cavities	32	32	33
Cavities per Period	2	2	3
Focusing Period ( $\beta_g\lambda$ )	14.5	15	18
Period Length (m)	3.02	4.30	6.33
No. of Cryostats	16	16	11
Total Length (m)	48.3	68.8	69.6

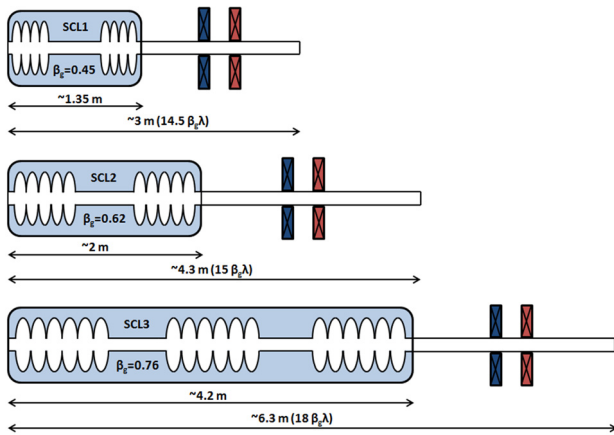


Figure 5: SCL Cryomodules.

The synchronous phase in SCL1 and SCL2 is set to -22 degrees and to -21 degrees in SCL3 (Figure 3). Each cavity family is designed for the same energy gain and beam power per cavity. As a result, the accelerating fields have to vary from cavity to cavity due to phase slips when  $\beta \neq \beta_g$ .

Transversally, the focusing is done with a doublet quadrupole arrangement located in the room temperature sections at the end of each cell. The six parameter matching between each SCL stage is found by varying six quadrupole gradients and the cavity phases at each transition region. After the SCL, an ~87 m long beam line with a final achromatic section will transport the beam to the ring.

### ONGOING STUDIES

Detailed beam dynamics studies are an integral part of the overall linac design development. Tracking simulations of the baseline model performed with Parmila [6] and TraceWin [7] indicate that the choice of tunes is such that the linac operates in the stable area of Hofmann's chart [8], thus avoiding space charge driven resonances, as it can be seen in Figure 6. An example of the beam envelope evolution throughout the linac when using a input waterbag distribution is shown in Figure 7, while Figure 8 shows the emittance evolution for the same input parameters.

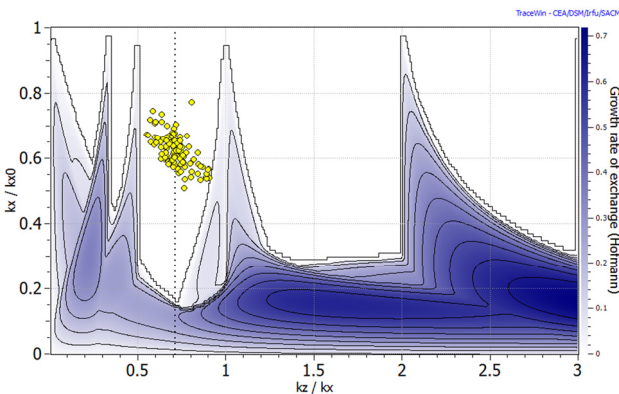


Figure 6: Linac working points on Hofmann's Stability Chart.

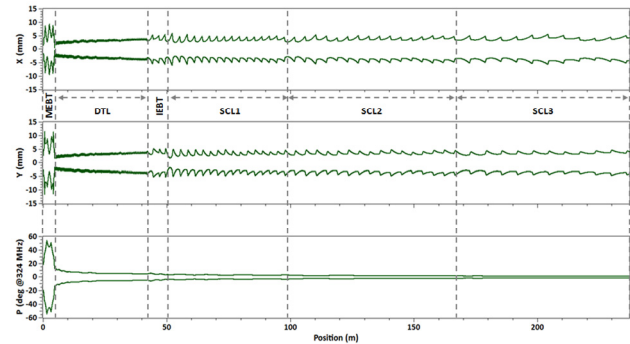


Figure 7: Linac beam envelopes (MEBT to SCL).

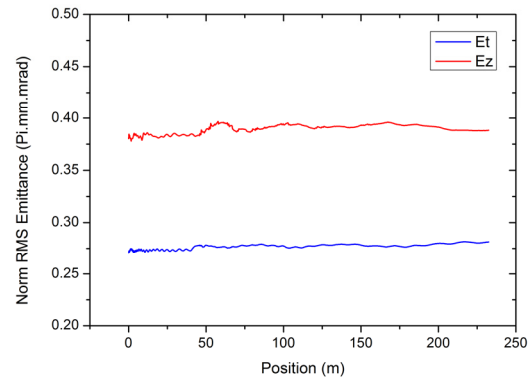


Figure 8: Linac emittance evolution (DTL to SCL).

In preparation for high power operation, one major research direction is understanding the transport of intense beams and the beam behaviour in the space-charge dominated regime, in particular halo formation. Halo is an important source of emittance growth that can eventually lead to beam loss and machine activation, a process that must be avoided in high intensity linacs. The latest advances in computing power will soon make possible simulations with entire particle populations, which is an essential tool in tackling halo formation and beam loss problems [9]. At RAL, current efforts are being put into running detailed end-to-end simulation studies on a local cluster using a parallel version of Impact [10] and 5 million macro-particles.

### REFERENCES

- [1] J. W. Thomason et al., Proc. of HB'08, WGE15.
- [2] G. Rees, "Linac, Beam Line and Ring Studies for an Upgrading of ISIS", RAL Internal Report, 2009.
- [3] G. Rees, Proc. of PAC'09, FR5REP086.
- [4] C. Plostinar et al., Proc. of IPAC'11, WEPC041.
- [5] A. Letchford et al., Proc. of IPAC'12, MOPPR056.
- [6] J. Billen et al., Proc. of LINAC'98, MO4047.
- [7] R. Duperrier, et al., Proc. of ICCS'02, p. 411.
- [8] I. Hofmann et al., Phys. Rev Lett. 86, 2313 (2001).
- [9] P. Ostroumov et al., Proc. of LINAC'08, TH301.
- [10] J. Qiang et al., Journal of Computational Physics, (163):434-451.